TECHNICAL PHYSICS LETTERS

15

Failure regions resembling geometrical shapes in sliding nanoindentation of Si-C-N thin films used for N/MEMS

© *R. Dash*[1], *A.S. Bhattacharyya*[1,2]

[1] Dept. of Nano Science and Technology, Central University of Jharkhand, Brambe, India
[2] Centre of Excellence in Green and Efficient Energy Technology (CoE GEET), Central University of Jharkhand, Brambe, India
E-mail: arnab.bhattacharya@cuj.ac.in, 2006asb@gmail.com

The failure regions during sliding nano indentation of technologically important SiCN thin films resembled geometrical shapes of Lemniscate and cardiod. An adhesive strength of 9 GPa was estimated. The failure followed two different stress regimes, one tangential responsible for the wear and the other axial responsible for the film/substrate adhesion. EDS spectra of the scratched region shown complete adhesive failure.

Keywords: sliding nanoindentation, SiCN thin films, adhesive strength

Sliding nanoindentation has been used to study the adhesion and wear properties of thin films. These studies are very significant for thin films used in devices based on Nano/Micro electro-mechanical systems (N/MEMS). The process consists of scratching the surface of the film with a ramping load and recording the tractional response till failure. The load at which the film fails is called the critical load. The nature of the film/substrate (level of hardness), the thickness of the films, loading rate, velocity, and stress in thin films are factors responsible [1].

Si-C-N thin films are popular because of their oxidation resistance, chemical inertness, piezoelectric properties, and microwave absorbing capabilities. They have been used extensively in N/MEMS, memory devices, electronic packaging, optoelectronic devices, and microwave absorption [2–11]. The nanocrystalline phases of SiC, Si_3N_4, and CNx are formed in Si-C-N [12].

The sliding indentation or nano scratch tests were done by Berkovich indenter present in the MTS (USA) nanoindentation equipment. In scratching, the probe is dragged across the sample surface keeping the force, rate, length, and angle of the scratch in control. The use of a lower load and smaller radius of the indenter increases surface sensitivity and also provides high contact pressure.

There are three contributions to the stress responsible for coating detachment: Elastic-plastic indentation stress, tangential friction stress, and internal stress. The failure of coating in scratch tests depends on the hardness of both the coating and the substrate. The critical load depends on many factors like the mechanical strength (adhesion, cohesion) of coating substrate composite, loading rate scratch speed, and indenter tip radius indenter material. The coating substrate-specific parameters that are important for scratch adhesion are mainly substrate hardness and
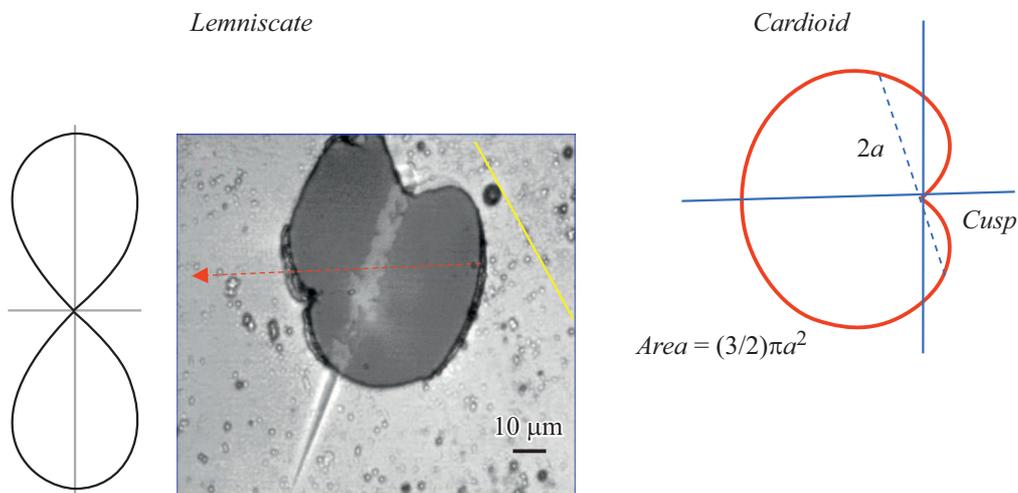

Figure 1. Lemniscate and Cardioid shaped failure zone during the scratch test

Full scale counts 2886   *Inside scratch track*

a

Element	K-ration	K-ration error	wt.%	wt.% error	at.%	at.% error
Si	0.002	± 0.000	0.32	± 0.03	0.62	± 0.07
Cr	0.191	± 0.002	16.67	± 0.15	17.70	± 0.16
Mn	0.019	± 0.001	1.94	± 0.10	1.95	± 0.10
Fe	0.715	± 0.004	73.05	± 0.40	72.20	± 0.39
Ni	0.073	± 0.001	8.01	± 0.16	7.53	± 0.15

Full scale counts 5002   *Coated zone*

b

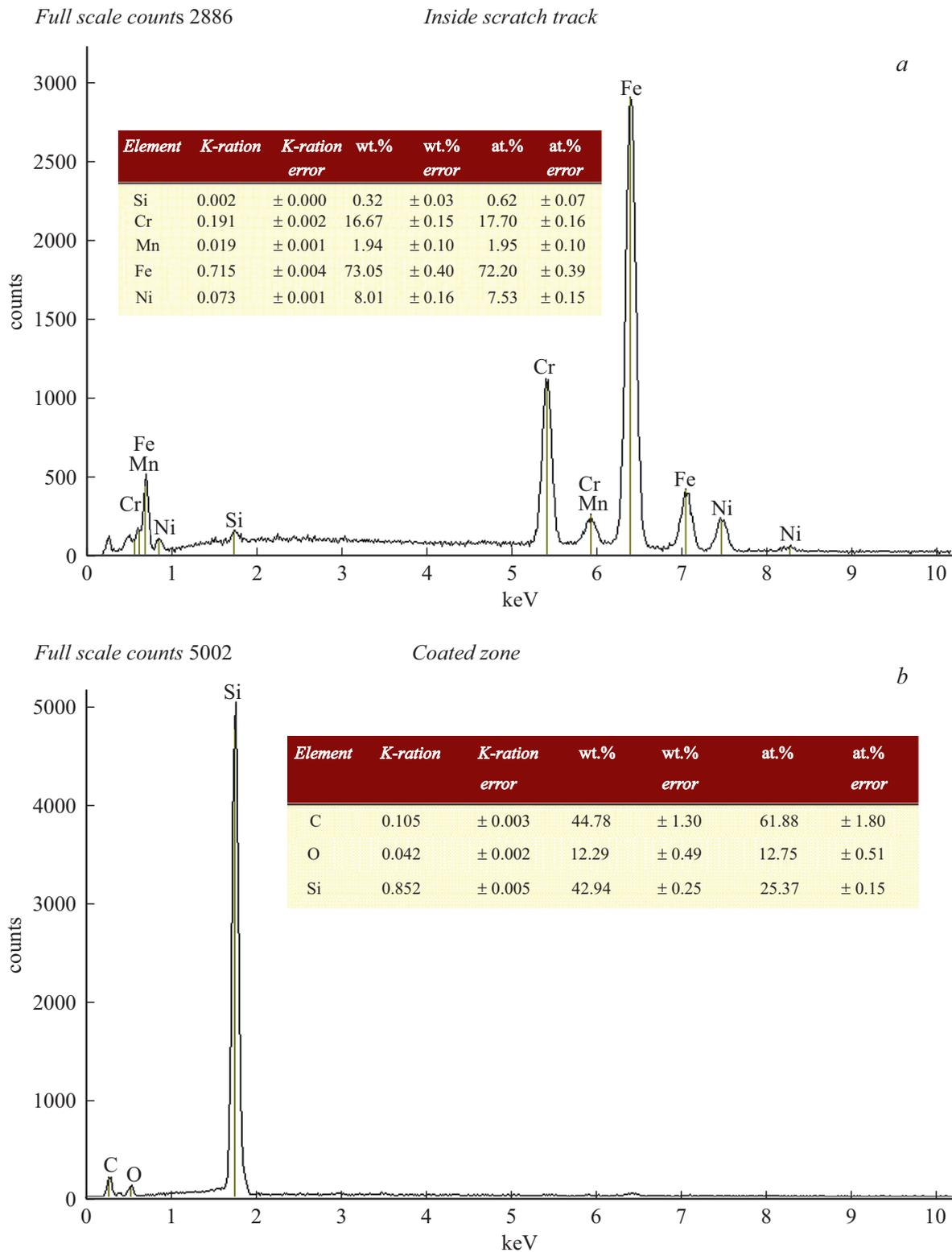| Element	K-ration	K-ration error	wt.%	wt.% error	at.%	at.% error
C	0.105	± 0.003	44.78	± 1.30	61.88	± 1.80
O	0.042	± 0.002	12.29	± 0.49	12.75	± 0.51
Si	0.852	± 0.005	42.94	± 0.25	25.37	± 0.15

Figure 2. EDS spectra of the a) scratch track and b) coated zone

roughness, coating thickness, frictional coefficients between coating and indenter, and internal stresses in the coating. The critical load however gets influenced by intrinsic factors (loading rate, scratch speed, tip radius, tip wear, and other machine factors) and extrinsic factors (substrate and coating hardness, modulus, surface roughness, friction) [13,14].

Static nanoindentations have been performed previously on these films and analysis of the fractured region has been

done in terms of geometrical shapes [15,16]. However, interestingly, sliding indentation which is not localized as in the case of static indentation has produced fractured regions which can also be related to geometrical shapes.

The appearance of two different zones of failure indicates the fact that there are two different aspects to sliding indentation failure one which is governed by the tangential stress causing the fractured region taking the shape of a cardioid is more related to the wear property of the coating, The axial stress just below the indenter is more related to the film/ substrate adhesion and creates a failure region resembling a lemniscate (Fig. 1).

Cardioid-shaped failure was also observed during scratch tests similar to that reported during static indentation (Fig. 1), which is due to the plastic zone near the crack tip which has grown in size due to overload. We can find the area of the failure region $\left(\frac{3}{2}\pi\,a^2\right)$ as per the geometry. The load applied was $50\,\mathrm{mN}$ which gives an approximate value of $9\,\mathrm{GPa}$ as the adhesive strength. The adhesive failure region inside the cardioid on the other hand resembles a Lemniscate ($r^2 = a^2 \cos 2\theta$). It consists of two equal loops, each symmetrical about the initial line, which divides each loop into two halves. The only difference we have in the scratch failure zone is that the number of lobes is not limited to two and extends further. The periodic closing of the loops is indicative of the fact that the stress responsible for fracture is periodic.

The stress distribution beneath the indenter during sliding indentation is much more complex than the static one and requires further study including dynamic Finite element modeling which we are working on.

EDS spectra of the scratch track with the corresponding atomic and weight % of different elements reveal the adhesive failure of the coating. The percentage of elements like 72.2 atom % Fe, 17.7 % Cr, 1.95 % Mn, etc as shown in Fig. 2 (a) indicates nothing but the SS304 whereas the spectra of the coated portion shown in Fig. 2 (b) is nothing but the elemental composition of the Si-C-N coating. Thus, on scratching the coating got completely removed exposing mere the stainless-steel substrate.

Acknowledgements

Conflict of interest

The authors declare that they have no conflict of interest.

References

[1] A.S. Bhattacharyya, Surf. Topogr.: Metrol. Prop., **9**, 035052 (2021). DOI: 10.1088/2051-672X/ac28aa

[2] J. Minming, X. Ke, L. Ningbo, Z. Beirong, Ceram. Int., **48** 2112 (2022). DOI: 10.1016/j.ceramint.2021.09.299

[3] I. Tanaka, S. Matuoka, Y. Harada, Diamond Relat. Mater.,**121**, 108732 (2022). DOI: 10.1016/j.diamond.2021.108732

[4] C. Jung, S. Song, H. Park, Y. Kim, E.J. Lee, S.G. Lee, H. Jeon, J. Vac. Sci. Technol. A, **39**, 042404 (2021). DOI: 0.1116/6.0000887

[5] N. Singh, K. Singh, D. Kaur, Ceram. Int., **43**, 8970 (2017). DOI: 10.1016/j.ceramint.2017.04.037

[6] N. Sigh, D. Kaur, Appl. Phys. Lett., **113**, 162103 (2018). DOI: 10.1063/1.5045723

[7] Y.-J. Choi, J.-H. Lee, J.-S. Choi, S.-J. An, Y.-M. Hwang, J.-S. Roh, K.-S. Im, Crystals, **11**, 489 (2021). DOI: 10.3390/cryst11050489

[8] J.-H. Lee, K.-S. Im, J.-H. Lee, IEEE J. Electron Dev. Soc., **9**, 728 (2021). DOI: 10.1109/JEDS.2021.3100760

[9] Q. Li, C. Chen, M. Wang, Y. Lv, Y. Mao, M. Xu, Y. Wang, X. Wang, Z. Zhang, S. Wang, W. Zhao, J. Stiens, J. Mater. Res. Technol., **15**, 460 (2021). DOI: 10.1016/j.jmrt.2021.08.043

[10] Q. Li, C. Chen, M. Xu, Y. Wang, X. Wang, Z. Zhang, W. Zhao, J. Stiens, Appl. Surf. Sci., **546**, 149121 (2021). DOI: 10.1016/j.apsusc.2021.149121

[11] S. Wang, H. Gong, Y. Zhang, M.Z. Ashfaq, Ceram. Int., **47**, 1302 (2021). DOI: 10.1016/j.ceramint.2020.08.250

[12] R. Riedal, H.-J. Kleebe, H. Schönfelder, F. Aldinger, Nature, **374**, 526 (1995). DOI: 10.1038/374526a0

[13] S.J. Bull, E.G. Berasetegui, Tribol. Int., **39**, 99 (2006). DOI: 10.1016/j.triboint.2005.04.013

[14] S.K. Mishra, A.S. Bhattacharyya, Mater. Lett., **62**, 398 (2008). DOI: 10.1016/j.matlet.2007.05.043

[15] A.S. Bhattacharyya, R.P. Kumar, S. Priyadarshi, Sonu, S. Shivam, S. Anshu, J. Mater. Eng. Perform., **27**, 2719 (2018). DOI: 10.1007/s11665-018-3289-7

[16] A.S. Bhattacharyya, R.P. Kumar, G. Acharya, V. Ranjan, Current Smart Mater., **2**, 39 (2017). DOI: 10.2174/2405465801666161130154515